Design and Development of an Ultrathin Triple Band Microwave Absorber Using Miniaturized Metamaterial Structure for Near-Unity Absorption Characteristics

Naveen Mishra[*] and Raghvendra Kumar Chaudhary

Abstract—This article discusses about the design and development of an ultrathin triple band microwave absorber using a miniaturized metamaterial structure for near-unity absorption characteristics. In order to design a miniaturized metamaterial (MTM) absorber unit cell with triple band response, two resonators, named as Structure-I and Structure-II, are configured within the single unit cell. The geometrical proportions of the suggested resonators have been chosen in such a manner so that Structure-I can contribute one absorption band while Structure-II can contribute two absorption bands. Therefore, the combination of two resonators offers triple band response with the highest absorption values of 99.04%, 99.62%, and 99.33% at the frequencies of 4.25 GHz, 8.35 GHz, and 11.06 GHz, respectively. Additionally, the suggested absorber unit cell claims miniaturization with total electrical size of $0.156\lambda_0 \times 0.156\lambda_0 \times 0.014\lambda_0$, where λ_0 corresponds to the free-space wavelength at the first peak absorption frequency of 4.25 GHz. Additionally, the electric field and vectored surface current distribution along with the input impedance graph has been used to discuss the absorption methodology of the suggested structure. Further, the MTM belongings of the suggested structure have been illustrated with the dispersion curve.

1. INTRODUCTION

Electromagnetic absorbers are passive devices which are utilized to absorb the incident electromagnetic wave. The historical background of the electromagnetic absorbers have been started from the Salisbury screen [1], Jaumann layer [2], Dallenbach layer [3] where the absorption of incident electromagnetic waves occur due to destructive interference. However, these electromagnetic absorbers have some major flaws such as large thickness and single absorption frequency which restrict their real time applications. In order to improve the absorption band of electromagnetic absorbers, carbon foam based pyramidal absorbers [4] become most popular. Until the present these absorbers have been utilized in anechoic chambers. However, large thickness becomes a major shortcoming of a pyramidal absorber, due to which it cannot be used for ultrathin applications. In order to reduce the thickness of electromagnetic absorbers, ferrite based absorbers [5, 6] have been addressed. However, this absorber is extremely bulky in nature and does not look like a better alternative for ultrathin applications.

In later years, a new kind of material, known as MTMs [7], grabs the attention of the microwave society. These materials are artificially designed and are homogeneous in nature. It can offer unconventional properties such as antiparallel group, phase velocities, and negative refractive index. These unconventional properties of MTMs have been exploited in various microwave applications such as super lenses [8], cloaking [9], antennas [10], filters [11], sensing [12, 13], harvesting [14, 15], and

absorbers [16, 17]. In the case of electromagnetic absorbers, the unconventional properties of MTMs are exploited to achieve miniaturization along with the ultrathin thickness and near unity absorption. The major advantage of such MTM absorbers is their controllable input impedance. In the case of MTM absorbers the input impedance can be altered by varying the geometrical proportions of the absorber unit cell. These absorbers are constituted with two metallic layers, between which a dielectric layer has been sandwiched. The upper metallic layer has a periodic organization of miniaturized frequency selective surfaces (FSS). The lower metallic layer is a plane copper surface which has been applied to restrain further propagation of the incident electromagnetic energy. Since the design mechanism of the MTM absorbers has been based on the resonant approach, these absorbers offer narrow bandwidth which becomes the major shortcoming of such absorber structures [17–20]. The problem of narrow bandwidth has restricted the application of MTM absorbers. With a specific end goal to enhance the operational bandwidth of such absorbers, several reports came into picture, which offer dual band [21, 22], triple band [23–26], and wideband [27–30] response. In this regard, mainly two approaches have been analysed. Among them, the first approach is based on the orthogonal arrangement of the scaled version of unit cell [23, 25]. This approach fruitfully improves the operational bandwidth of MTM absorbers. However, the shortcoming of this approach is its larger unit cell size. In another approach, the unit cell has been designed with multi-resonators within a single unit cell [22, 27]. Further, this work is inspired by the article [31], where two different kinds of resonators are used to generate triple band response. In [31], study has been done for an outer rectangular ring which is diagonally split while in the present suggested work, study has been done for a circular ring which is diagonally split.

In this article, the design and development of an ultrathin triple band microwave absorber using a miniaturized metamaterial structure for near-unity absorption characteristics are discussed. The suggested absorber unit cell has been configured with the two resonators termed as Structure-I and Structure-II. In the triple band response of the suggested absorber configuration, one absorption band (at the frequency of 8.35 GHz) has been initiated due to Structure-I while the other two absorption bands (at 4.25 GHz and 11.06 GHz) have been originated from Structure-II. The electrical excitation of the upper metallic layer (periodic arrangement of resonators or FSS) and magnetic excitation of dielectric material (sandwiched between upper and lower metallic layers) have been discussed to explain the absorption methodology of the suggested absorber structure. In addition, the suggested absorber structure is capable to offer polarization independence property which is further explained with the four-fold structural symmetry of the suggested unit cell.

2. ABSORBER DESIGN AND ANALYSIS

The layout of the suggested unit cell with its proportions in caption is presented in Fig. 1. It is evident that two resonators termed as Structure-I and Structure-II have been merged to form the suggested triple band absorber unit cell. Structure-I is configured with four rectangular split ring resonators which
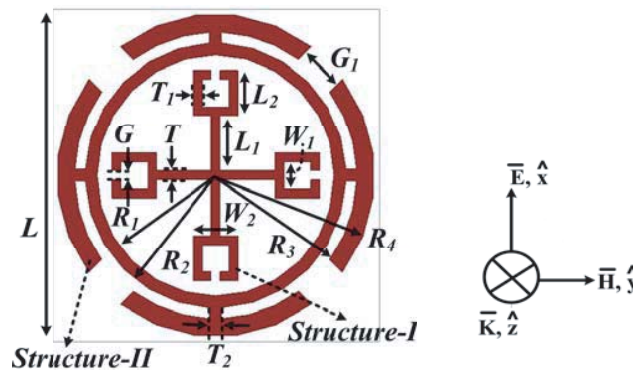
Figure 1. Layout of the suggested unit cell. [All proportions are in mm: $L = 11$, $L_1 = 1.85$, $L_2 = 1.5$, $W_1 = 0.9$, $W_2 = 1.5$, $T = 0.3$, $T_1 = 0.3$, $T_2 = 0.4$, $G = 0.3$, $G_1 = 1.06$, $R_1 = 4$, $R_2 = 4.4$, $R_3 = 4.75$, $R_4 = 5.35$].

are connected to each other by thin strip lines, forming a plus shaped structure whose all four ends are connected with the rectangular split ring resonators. Apart from Structure-I, Structure-II has been configured with two rings where the outer ring is divided diagonally in four parts, and all these divided parts are connected with an inner ring with the four distinct thin strip lines. In order to design the suggested absorber structure, a two-sided copper laminated FR-4 epoxy substrate (dielectric constant 4.4, loss tangent of 0.02) with thickness of 1 mm has been used. Further, both the resonators have been etched on the upper copper coating of thickness 35 μm. The lower side of substrate material is also covered with a 35 μm thick copper sheet. This sheet is used to restrain the onward propagation of the incident electromagnetic energy. The complete analysis for the suggested absorber structure has been conducted on the HFSS 14.0 3-D simulation software. In this process, master-slave boundary along with floquet port excitation has been applied. The absorptivity of the suggested absorber configuration has been computed mathematically by Eq. (1).

$$A = 1 - |S_{11}|^2 - |S_{21}|^2 \tag{1}$$

Here $|S_{11}|^2$ and $|S_{21}|^2$ stand for the reflected and transmitted powers, respectively.

Further, the copper layer present on the lower side of the dielectric material restricts the transmission of incident electromagnetic wave which results in zero transmitted power and due to this Eq. (1) shrinks into Eq. (2).

$$A = 1 - |S_{11}|^2 \tag{2}$$

Figure 2 demonstrates the absorption response for Structure-I and Structure-II independently. It can be observed that Structure-I contributes one absorption band with peak absorptivity of 98.80% at the frequency of 8.57 GHz while Structure-II contributes dual-band response with peak absorptivities of 97.67% and 99.22% at the frequencies of 4.31 and 11.06 GHz, respectively. Further, the two resonators are combined to form the suggested unit cell whose reflectance and absorption response are depicted in Fig. 3. It is evident that the suggested absorber structure offers a triple band response with peak absorptivities of 99.04%, 99.62%, and 99.33% at the frequencies of 4.25, 8.35, and 11.06 GHz, respectively. The above two figures (Fig. 2 and Fig. 3) clearly show that after combining the two resonators (suggested unit cell), the absorption peaks are shifted towards lower frequency. This shift in absorption frequency has been explained with the coupling between the two resonators. It has also been observed that the suggested absorber structure offers zero reflectance and near unity absorption at all the three absorption peaks. The electrical footprint area of the suggested absorber structure is $0.156\lambda_0 \times 0.156\lambda_0 \times 0.014\lambda_0$, where λ_0 corresponds to the free-space wavelength at 4.25 GHz. Additionally the suggested absorber structure offers simulated full width at half maximum bandwidth of 190 (4.15–4.34 GHz), 340 (8.18–8.52 GHz), and 410 (10.85–11.26 GHz) MHz.
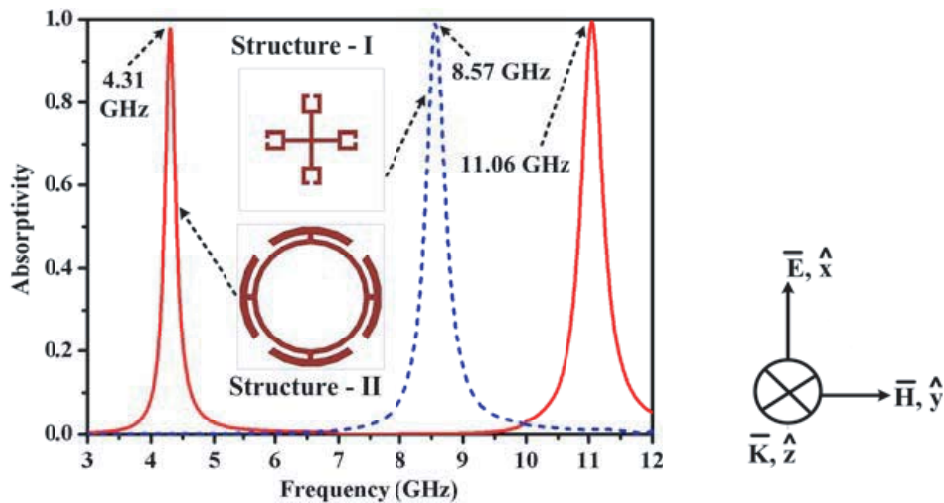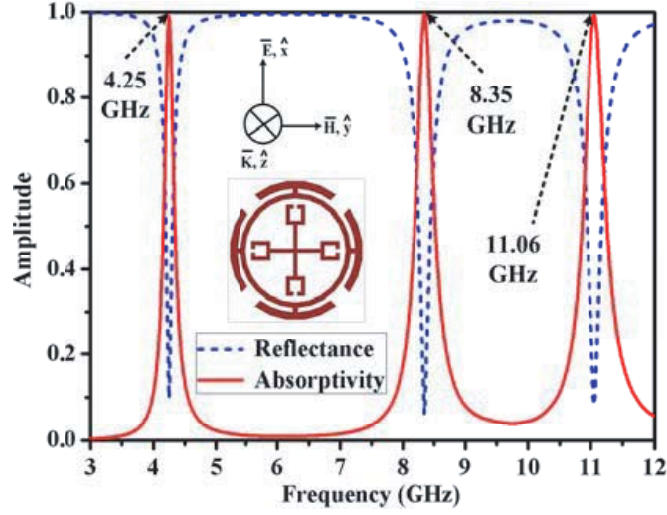

**Figure 2.** Individual simulated absorption response for Structure-I and Structure-II.

Figure 3. Simulated reflectance and absorption plots for suggested absorber structure.

2.1. Discussion on the Dispersion Characteristics of the Suggested Absorber Structure

The dispersion characteristics of the suggested absorber unit cell is determined with Eq. (3) [32] and presented in Fig. 4. This analysis has been carried out to approve the MTM characteristics for the suggested unit cell. Further, the plotted dispersion characteristic has been categorized in two regions, and among them, one is known as right-handed (RH) region and the other known as left-handed (LH) region. In LH region, the slope of the graph must be negative which means that it allows antiparallel phase and group velocities. Apart from the LH region, the dispersion graph shows positive slope in RH region which allows parallel group and phase velocities.

$$\beta d = \cos^{-1}\left(\frac{1 - S_{11}S_{22} + S_{12}S_{21}}{2S_{21}}\right) \tag{3}$$
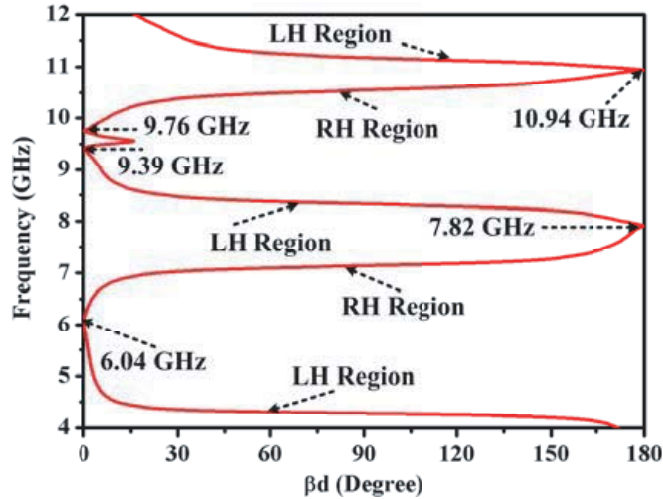
Figure 4. Dispersion characteristics for the suggested unit cell.

In the plotted dispersion curve, the first two absorption (4.15–4.34 GHz and 8.18–8.52 GHz) bands lie in the LH region. The third absorption band (10.85–11.26 GHz) can be divided into two parts, and the first part (10.85–10.94 GHz) lies in the RH regions while the second part (10.94–11.26 GHz) lies in the LH region.

2.2. Discussion on the Dispersion Characteristics of the Suggested Absorber Structure

This section discusses the absorption methodology of the suggested absorber structure. In this regard, the normalized input impedance plot is depicted in Fig. 5. It is a well-known fact that the reflection from any surface can be reduced to zero by making the input impedance of the surface identical to the free space impedance $((377 + j0)\ \Omega)$. It can be observed that with the optimized dimensions of the suggested absorber structure, the input impedances at all three peak absorption frequencies become
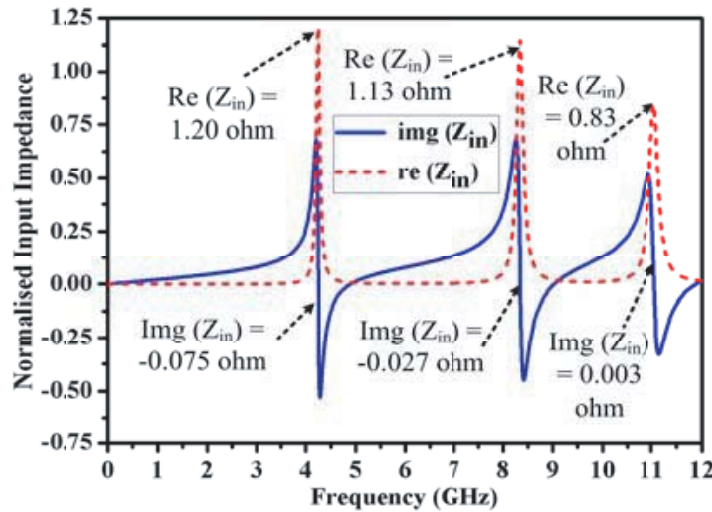

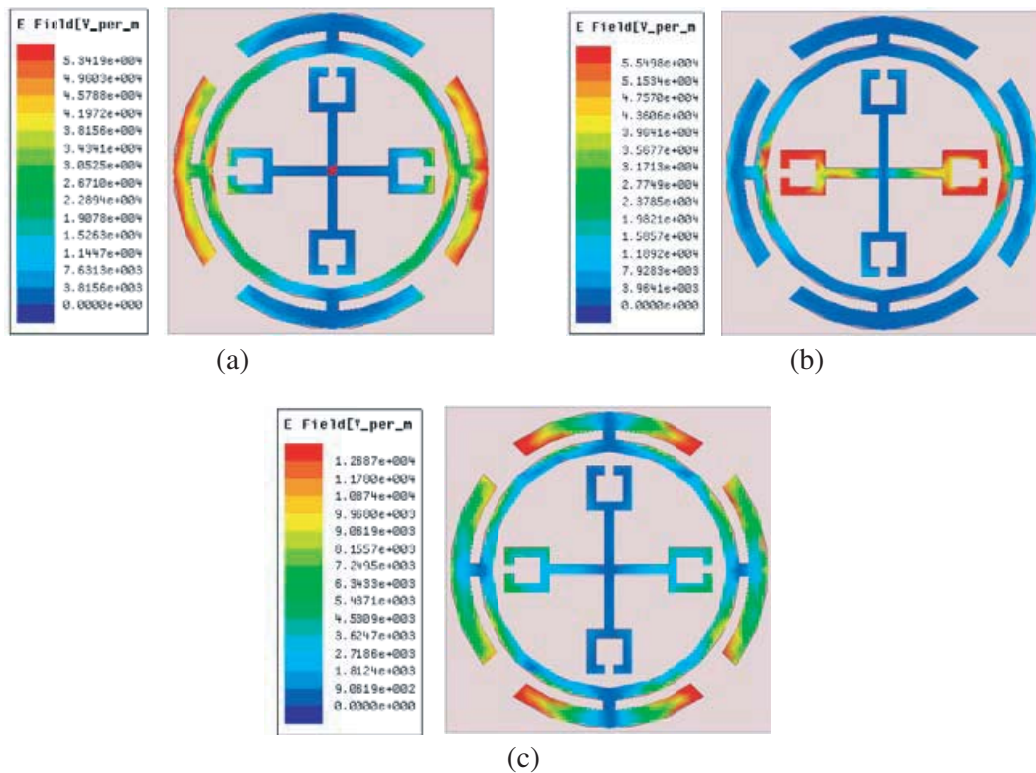**Figure 5.** Normalized input impedance curve for the suggested triple band absorber configuration.
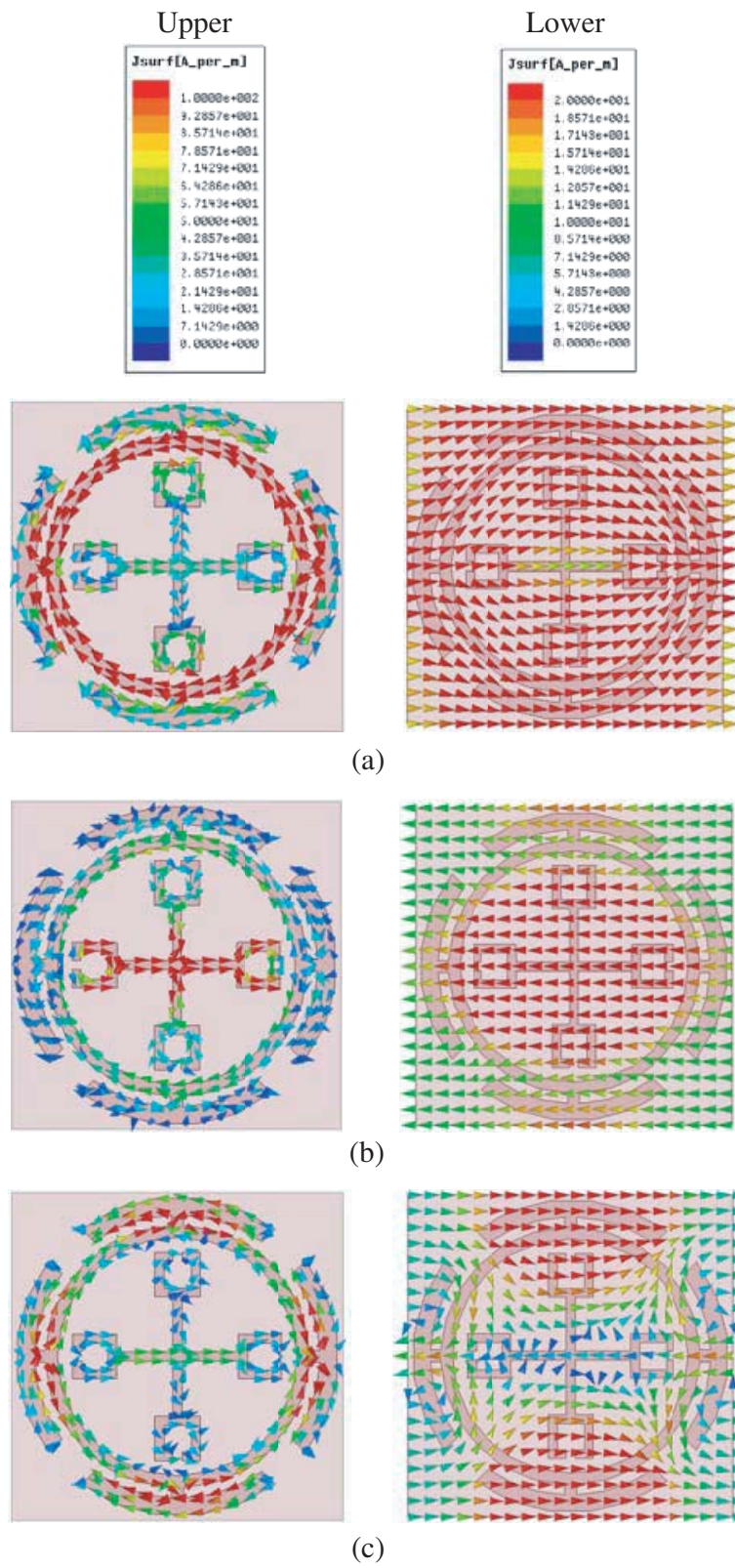

(a)

(b)

(c)

Figure 6. Electric field distribution plot at all three peak absorption frequencies of the suggested triple band absorber.

Upper   Lower

(a)

(b)

(c)

Figure 7. Surface current distribution plot at all three absorption peaks of the suggested triple band absorber structure.

near free space impedance. This results in the least amount of reflection from the surface at all three absorption peaks. Because of this, at all three peak absorption frequencies, near unity absorption has been achieved. The input impedance of any surface can be mathematically calculated by Eq. (4) [33].

$$Z_{in} = \sqrt{\frac{(1 + S_{11})^2 - (S_{21})^2}{(1 - S_{11})^2 - (S_{21})^2}} \qquad (4)$$

Further the absorption methodology of the suggested absorber structure has also been discussed with the electric and magnetic excitations. In this analysis, surface current distribution and electric field distribution are utilized. The electric field concentrations on the surface of the suggested triple band configuration at all three peak absorption frequencies of 4.25, 8.35, and 11.06 GHz are depicted in Figs. 6(a), (b), and (c), respectively. It can be observed that the maximum electric field concentrations at the first and third absorption peaks are on Structure-II. Similarly, at the second absorption peak, the maximum field concentration is on Structure-I. These electric field concentrations are accountable for the origination of electrical excitation.

Similar to electric field distribution, the surface current distributions at all three absorption peaks of 4.25. 8.35, and 11.06 GHz are depicted in Figs. 7 (a), (b), and (c), respectively. Figs. 7(a) and (c) clearly show that the maximum surface current distributions at the absorption peaks of 4.25 and 11.06 GHz are on Structure-II while the maximum surface current concentration at the frequency of 8.35 GHz is on Structure-I. Additionally, it can also be observed that the directions of surface current at all three absorption peaks in the upper and lower metallic layers make a circulating current which is accountable for the magnetic excitation. This simultaneous occurrence of electric and magnetic excitation is responsible for the origination of all three absorption peaks.

2.3. Effect of Polarization and Incidence Angle Variation on Absorption Coefficient

The absorption response, at distinct polarization angles, under normal incidence of electromagnetic energy is presented in Fig. 8. It is evident that under normal incidence of electromagnetic energy the variation in polarization angle does not affect the absorption coefficient which confirms the polarization independence property of the suggested MTM absorber structure. The polarization independent behaviour of the suggested configuration can be theoretically clarified with the four-fold structural symmetry of the suggested structure. During this analysis, the direction of wave propagation remains settled, and the directions of E field and H filed start turning with the angle of ϕ degrees. In this study, the polarization angle ϕ is varied from $0°$ to $90°$ at a step size of $15°$.
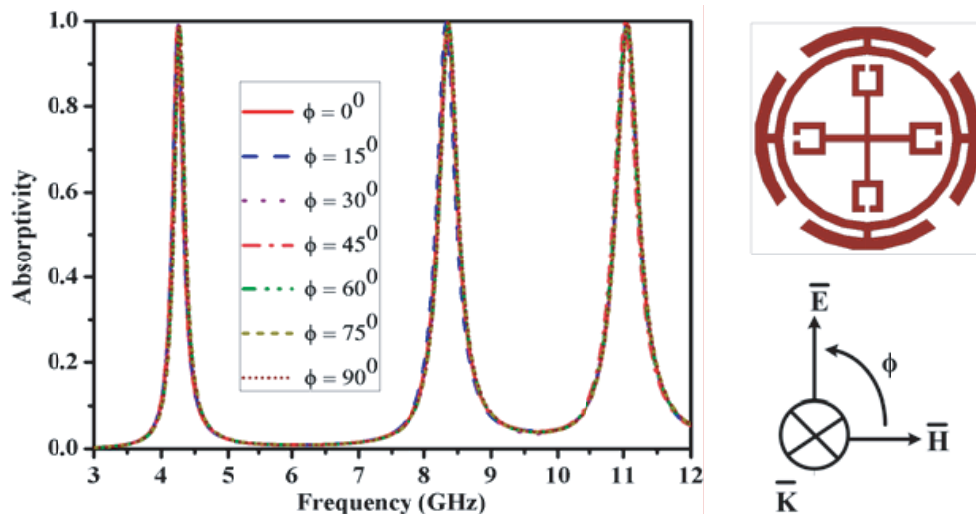
Figure 8. Simulated absorptivity response for suggested absorber structure at distinct polarization angles.
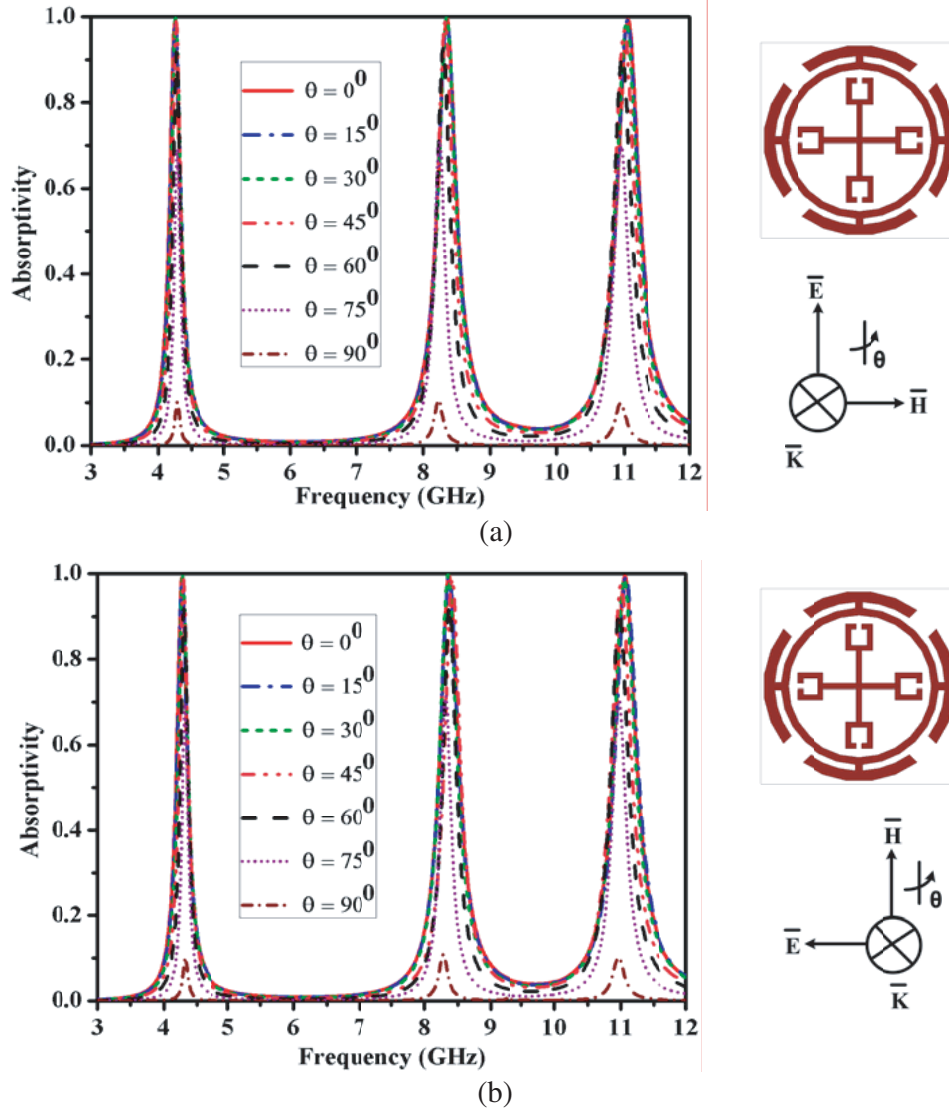
Figure 9. Simulated absorptivity response for suggested absorber structure at distinct incidence angles. (a) TE polarization state. (b) TM polarization state.

Further, the effect of incidence angle (θ) variation on the absorption response for the suggested absorber configuration is depicted in Fig. 9. In this study, the absorptivities are analysed under transvers electric (TE) and transvers magnetic (TM) polarization states by varying incidence angle θ from 0° to 90° at a step size of 15° and are depicted in Figs. 9(a) and (b), respectively. It is observed that the suggested absorber structure, under both the polarization states up to 60° incidence angle, offers more than 80% absorptivity. In the analysis of TE polarization state, the electric field vector remains settle while the magnetic field vector and direction of wave propagation rotate with the incidence angle of θ. Similar to TE polarization state in the case of TM polarization, the magnetic field vector remains stationary, and the electric field vector along with direction of wave propagation rotates with the incidence angle of θ. It can also be observed that under both polarization states with the increment in incidence angle from 0° to 90°, the absorptivity decreases. This can be explained with the reduction in electric and magnetic excitations. In TE polarization with the rotation of magnetic field vector, the magnetic excitation decreases which results in reduction of absorptivity at distinct incidence angles. In a similar manner under TM polarization, the rotating electric field vector corresponds to low electric excitation and causes reduction in absorptivity.

3. EXPERIMENTAL RESULTS

In order to verify the absorption response of the suggested absorber configuration, a prototype has been fabricated which is shown in Fig. 10. In this process, a 1 mm thick FR-4 epoxy substrate is used. The substrate material should be laminated on both sides with a 35 µm thick copper layer. On the upper copper layer, the suggested unit cell is printed in the form of a 25×25 array. Further, the absorption measurement for the fabricated proto-type is executed with two similar horn antennas of desired frequency spectrum and PNA vectored network analyzer (Agilent N5221A). In this measurement setup, any horn antenna from the selected two horn antennas can be employed for transmission and reception purposes. The layout of the ideal measurement setup for measuring absorption coefficient is depicted in Fig. 11(a). Further, the real time measurement setup used for measuring absorption, only under oblique incidence angle, is shown in Fig. 11(b).
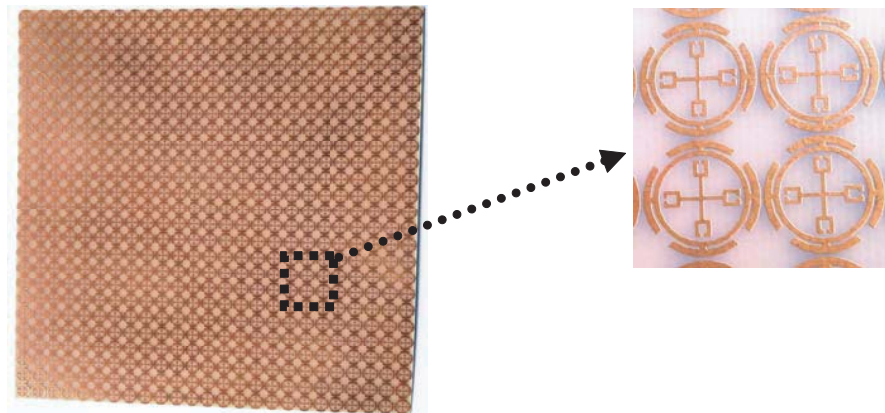
Figure 10. Fabricated proto-type of the suggested triple band MTM absorber.
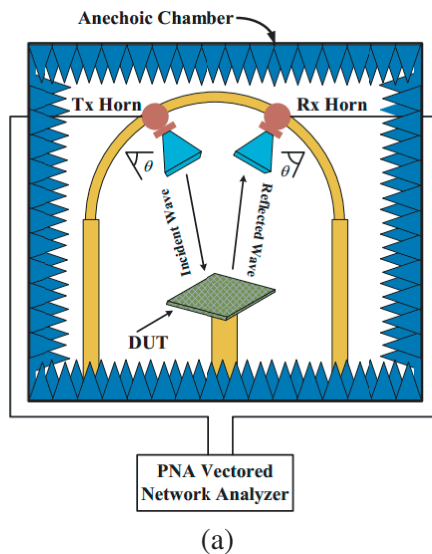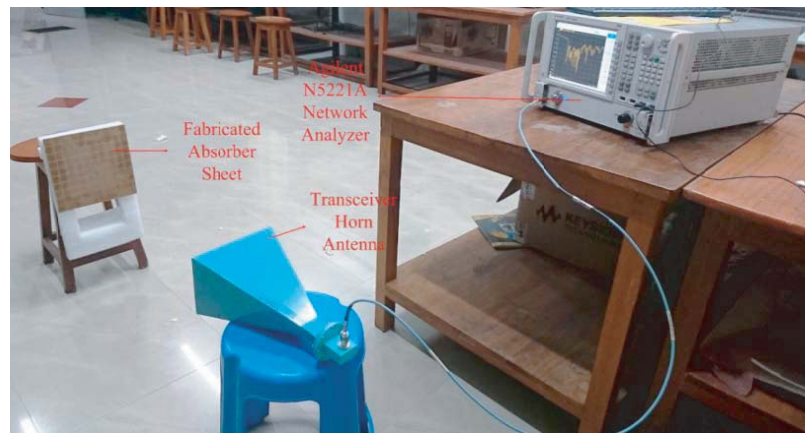
(a)   (b)

Figure 11. Absorption measurement setup. (a) Layout of ideal measurement setup. (b) Real environment measurement setup.

In the beginning of absorption measurement, first of all a reference input reflection coefficient is estimated. In this regard, a metallic (copper) plate is placed in front of the pair of horn antennas, and input reflection coefficient is estimated. This estimated input reflection coefficient is treated as reference. A similar approach has been utilized to estimate the input reflection coefficient for the
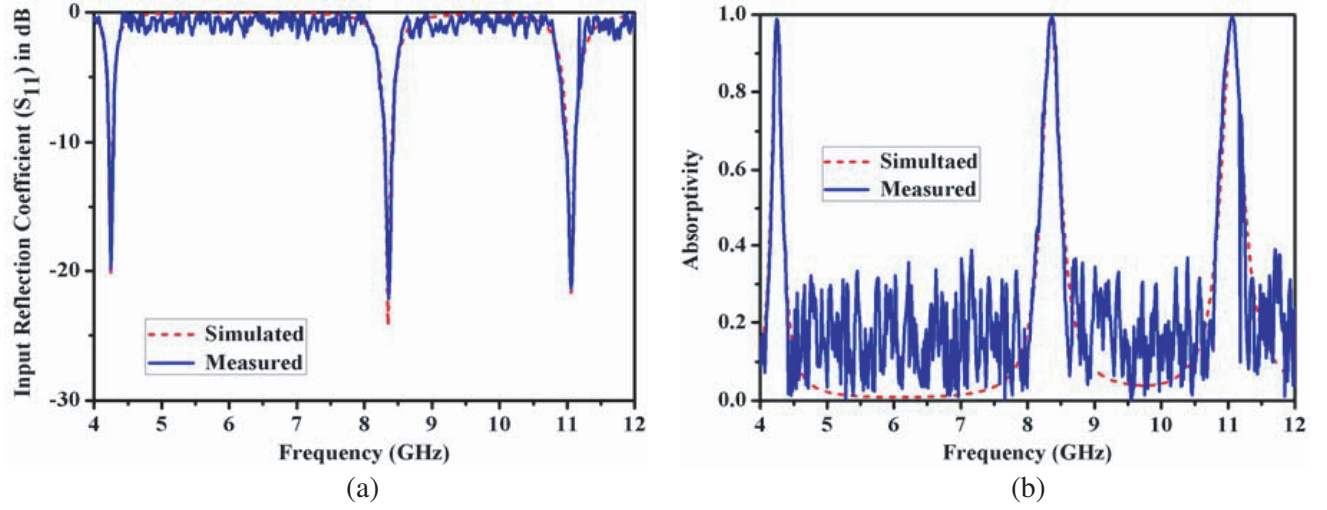
Figure 12. Simulated and measured responses for the suggested triple band MTM absorber structure. (a) Input reflection coefficient, (b) absorptivity.

experimentally developed proto-type. In order to eliminate the surrounding effect, estimated value of reference input reflection coefficient is subtracted from the estimated input reflection coefficient of proto-type. The difference between the two input reflection coefficients is termed as normalized input reflection coefficient. This normalized input reflection coefficient is substituted in Eq. (2) to calculate the absorptivity of fabricated proto-type. Fig. 12 illustrates the simulated and estimated values of input reflection coefficient (Fig. 12(a)) and absorptivity (Fig. 12(b)) responses for the suggested triple band MTM absorber structure. It can be observed that the measured and simulated responses show proper concurrence with each other except the occurrence of ripples, out of the absorption bands. This deviation may occur due to the measurement in open surrounding. The measured result shows a triple band response with peak absorptivities of 98.96%, 99.39%, and 99.27% at the frequencies of 4.26, 8.37, and 11.06 GHz, respectively.

A small deviation has been observed between the simulated and measured absorption peaks. This deviation may be because of the non-uniformity of the substrate material. Further, the suggested structure provides measured full width at half maximum (FWHM) bandwidth of 180 (4.16–4.34 GHz), 330 and (8.18–8.51 GHz) 400 (10.84–11.24 GHz) MHz in all three absorption bands. Additionally, Table 1 depicts the performance comparison of the suggested absorber structure with the earlier reported works.

Table 1. Comparison of the performance of the suggested work with earlier published works.

Parameters	This work	[23]	[24]	[25]	[26]
UCS* (mm^3)	$11 \times 11 \times 1$	$15 \times 15 \times 1$	$18 \times 18 \times 1$	$18 \times 18 \times 1.5$	$28.2 \times 28.2 \times 1.6$
LAP*	4.25	7.46	5.22	3.07	4.2
UCS with respect to LAP (λ_0)	$0.156 \times 0.156 \times 0.014$	$0.37 \times 0.37 \times 0.024$	$0.31 \times 0.31 \times 0.017$	$0.184 \times 0.184 \times 0.015$	$0.398 \times 0.398 \times 0.022$
Bands	Three	Three	Three	Three	Three

* UCS — Unit cell size, LAP — Lowest absorption peak.

4. CONCLUSION

In this article the design and development of an ultrathin triple band microwave absorber using miniaturized metamaterial structure for near-unity absorption characteristics has been presented. There are two resonators termed as Structure-I and Structure-II which are merged to form the suggested triple band absorber unit cell. Structure-I is accountable for the origination of the second absorption band while Structure-II is responsible for the first and third absorption bands. In order to confirm the MTM characteristics of the suggested ultrathin triple band absorber, the dispersion characteristics are utilized. The suggested absorber structure offers triple band response with the highest absorption values of 99.04%, 99.62%, and 99.33% at the absorption peaks of 4.25 GHz, 8.35 GHz, and 11.06 GHz, respectively. Further, it also claims miniaturization with a complete electrical footprint area of $0.156\lambda_0 \times 0.156\lambda_0 \times 0.014\lambda_0$, where λ_0 corresponds to the free-space wavelength at the first absorption peak of 4.25 GHz. Additionally, the absorption methodology for the suggested absorber structure has been discussed with the electric field and vectored surface current distribution plot. It can also be discussed with the input impedance curve.

REFERENCES

1. Salisbury, W. W., "Absorbent body for electromagnetic waves," U.S. Patent 2599944, filled May 11, 1943, granted June 10, 1952.
2. Cheldavi, A. and M. Kamarei, "Optimum design of n sheet capacitive Jaumann absorber using genetic algorithm," *IEEE International Symposium on Antenna and Propagation*, Vol. 4, 2296–2299, Montreal, Quebec, Canada, July 13–18, 1997.
3. Chambers, B. and A. Tennant, "Active Dallenbach radar absorber," *IEEE International Symposium on Antennas and Propagation*, 381–384, Albuquerque, New Mexico, USA, July 9–14, 2006.
4. Ishihara, K. and Y. Tomiyama, "Electromagnetically anechoic chamber and shield structure therfor," US Patent 5134405, filed February 27, 1989, granted July 28, 1992
5. Singh, P., V. K. Babbar, A. Razdan, R. K. Puri, and T. C. Goel, "Complex permittivity, permeability, and X-band microwave absorption of CaCoTi ferrite composites," *Journal of Applied Physics*, Vol. 87, No. 9, 4362–4366, 2000.
6. Parida, R. C., D. Singh, and N. K. Agarwal, "Implementation of multilayer ferrite radar absorbing coating with genetic algorithm for radar cross-section reduction at X-band," *Indian Journal of Radio and Space Physics*, Vol. 36, 145–152, 2007.
7. Caloz, C. and T. Itoh, *Electromagnetic Metamaterials: Transmission Line Theory and Microwave Applications*, John Wiley & Sons, 2006.
8. Fang, N., H. Lee, C. Sun, and X. Zhang, "Sub-diffraction-limited optical imaging with a silver super lens," *Science*, Vol. 308, 534–537, 2005.
9. Schurig, D., J. J. Mock, B. J. Justice, S. A. Cummer, J. B. Pendry, A. F. Starr, and D. R. Smith, "Metamaterial electromagnetic cloak at microwave frequencies," *Science*, Vol. 314, 977–980, 2006.
10. Mishra, N. and R. K. Chaudhary, "A miniaturized ZOR antenna with enhanced bandwidth for WiMAX applications," *Microwave and Optical Technology Letters*, Vol. 58, 71–75, 2016.
11. Fouad, M. A. and M. A. Abdalla, "New π-T generalised metamaterial negative refractive index transmission line for a compact coplanar waveguide triple band pass filter applications," *IET Microw. Antennas Propag.*, Vol. 8, 1097–1104, 2014.
12. Akgol, O., O. Altintas, E. E. Dalkılınc, E. Unal, M. Karaaslan, and C. Sabah, "Metamaterial absorber-based multisensor applications using a meander-line resonator," *Optical Engineering*, Vol. 56, No. 8, 087104, 2017.

13. Bakır, M., M. Karaaslan, E. Unal, O. Akgol, and C. Sabah, "Microwave metamaterial absorber for sensing applications," *Opto-Electronics Review*, Vol. 25, No. 4, 318–325, 2017.

14. Ünal, E., M. Bağmancı, M. Karaaslan, O. Akgol, H. T. Arat, and C. Sabah, "Zinc oxide-tungsten-based pyramids in construction of ultra-broadband metamaterial absorber for solar energy harvesting," *IET Optoelectronics*, Vol. 11, No. 3, 114–120, 2017.

15. Bağmancı, M., M. Karaaslan, O. Altıntaş, F. Karadağ, E. Tetik, and M. Bakır, "Wideband metamaterial absorber based on CRRS with lumped elements for microwave energy harvesting," *Journal of Microwave Power and Electromagnetic Energy*, Vol. 52, No. 1, 45–59, 2018.

16. Bilotti, F., L. Nucci and L. Vegni, "An SRR based microwave absorber," *Microwave and Optical Technology Letters*, Vol. 48, No. 11, 2171–2175, 2006.

17. Landy, N. I., S. Sajuyigbe, J. J. Mock, D. R. Smith, and W. J. Padilla, "Perfect metamaterial absorber," *Physical Review Letters*, Vol. 100, No. 20, 207402, 2008.

18. Wang, B., T. Koschny, and C. M. Soukoulis, "Wide-angle and polarization-independent chiral metamaterial absorber," *Phys. Rev. B*, Vol. 80, 033108, 2009.

19. Thummaluru, S. R., N. Mishra, and R. K. Chaudhary, "Design and analysis of an ultra-thin X-band polarization — Insensitive metamaterial absorber," *Microwave and Optical Technology Letters*, Vol. 58, 2481–2485, 2016.

20. Kalraiya, S., R. K. Chaudhary, M. A. Abdalla, and R. K. Gangwar, "Polarization and incident angle independent metasurface absorber for X-band application, material research express," *IOP Sciences*, Vol. 6, No. 4, 045802, 2019.

21. Zhai, H., Z. Li, L. Li, and C. Liang, "A dual-band wide-angle polarization-insensitive ultrathin gigahertz metamaterial absorber," *Microwave and Optical Technology Letters*, Vol. 55, 1606–1609, 2013.

22. Kumari, K., N. Mishra, and R. K. Chaudhary, "An ultra-thin compact polarization insensitive dual band absorber based on metamaterial for X-band applications," *Microwave and Optical Technology Letters*, Vol. 59, No. 10, 2664–2669, 2017.

23. Li, H., L. H. Yuan, B. Zhou, X. P. Shen, Q. Cheng, and T. J. Cui, "Ultrathin multiband gigahertz metamaterial absorbers," *Journal of Applied Physics*, Vol. 110, 014909, 2011.

24. Bhattacharyya, S., S. Ghosh, and K. V. Srivastava, "Triple band polarization-independent metamaterial absorber with bandwidth enhancement at X-band," *Journal of Applied Physics*, Vol. 114, 094514, 2013.

25. Bian, B., S. Liu, S. Wang, X. K. Kong, H. Zhang, B. Ma, and H. Yang, "Novel triple band polarization-insensitive wide-angle ultra-thin microwave metamaterial absorber," *Journal of Applied Physics*, Vol. 114, 194511, 2013.

26. Thummaluru, S. R., N. Mishra, and R. K. Chaudhary, "Design and analysis of an ultrathin triple-band polarization independent metamaterial absorber," *AEU — International Journal of Electronics and Communications*, Vol. 82, 508–515, 2017.

27. Lee, J. and S. Lim, "Bandwidth enhanced and polarization-insensitive metamaterial absorber using double resonance," *Electronics Lett.*, 47, 2011.

28. Ding, F., Y. Cui, X. Ge, Y. Jin, and S. He, "Ultra-broadband microwave metamaterial absorber," *Applied Physics Letters*, Vol. 100, 103506, 2012.

29. Soheilifar, M. R. and R. A. Sadeghzadeh, "Design, simulation, and fabrication of an ultrathin planar microwave metamaterial absorber," *Microwave and Optical Technology Letters*, Vol. 56, 2916–2922, 2014.

30. Ghosh, S., S. Bhattacharyya, and K. V. Srivastava, "Bandwidth enhancement of an ultrathin polarization insensitive metamaterial absorber," *Microwave and Optical Technology Letters*, Vol. 56, 350–355, 2014.

31. Mishra, N., D. K. Choudhary, R. Chowdhury, K. Kumari, and R. K. Chaudhary, "An investigation on compact ultra-thin triple band polarization independent metamaterial absorber for microwave frequency applications," *IEEE Access*, Vol. 5, 4370–4376, 2017.

32. Mehdipour, A., T. A. Denidni, and A. R. Sebak, "Multi-band miniaturized antenna loaded by ZOR and CSRR metamaterial structures with monopolar radiation pattern," *IEEE Transactions on Antennas and Propagation*, Vol. 62, 555–562, 2014.

33. Smith, D. R., D. C. Vier, T. Koschny, and C. M. Soukoulis, "Electromagnetic parameter retrieval from inhomogeneous metamaterials," *Physics Review E*, Vol. 71, 036617, 2005.